Astron. Astrophys. 364, 179–190 (2000)

ASTRONOMY AND ASTROPHYSICS

Spots and plages on a young main-sequence solar-type star: HD 206860⋆

A. Frasca[1], **R. Freire Ferrero**[2], **E. Marilli**[1], **and S. Catalano**[1]

[1] Osservatorio Astrofisico di Catania, via S. Sofia 78, 95125 Catania, Italy
[2] Observatoire Astronomique, 11 rue de l'Université, 67000 Strasbourg, France

Received 20 June 2000 / Accepted 18 October 2000

Abstract. The young solar type star HD 206860 is known to be a photometric variable with emission in the core of Ca II H & K lines, several times more intense than the Sun when observed as a star.

The photometric and spectroscopic monitoring of HD 206860 from near contemporaneous observations at Serra La Nave (Catania, Italy) and at the Observatoire de Haute Provence (OHP, France) shows that chromospheric spectral-line flux and photometric variations follow the same period (4.74 days).

From Strömgren photometry and Ca II and Hα chromospheric emission clearly anti-correlated variations have been found.

This result suggests that spots and plages in this single solar-type star are spatially associated, as frequently observed for the largest sun-spot groups and for some very active RS CVn systems.

A spot/plage model applied to the observed flux curves allows a crude reconstruction of the 3D structure of the external atmosphere of this star.

Key words: stars: activity – stars: individual: HD 206860

1. Introduction

In the Sun, when both faculae and sunspots are observed, it is found that spots are invariably associated with faculae, although the reverse is not always the case. Faculae generally forecast the occurrence of a centre of activity before a spot develops and survive for some time after the disappearance of the spot (see e.g. Priest 1982, and references therein). Therefore active regions trace magnetic flux tube emersion (Zirin 1988). During their buoyant rise to the surface, flux tubes are influenced by several effects, such as the Coriolis force, magnetic tension, drag, and convective motions. Studies of the motion and orientation of active region manifestations (spots, plages, etc.) will provide relevant information about the relative importance of these forces, and thus on the physical processes and conditions beneath the surface. This piece of information appears to be of great importance in understanding the magnetic field origin and the cycle mechanism of the Sun and sun-like stars.

In many active RS CVn binaries long-term spectral monitoring campaigns in the Hα region have revealed rotational modulation due to surface inhomogeneities at chromospheric level (Frasca et al. 1998).

Simultaneous photometric and spectroscopic observations have shown that the solar-like scenario of spatial association between spots and plages applies to these evolved and extremely active stars (Rodonò et al. 1987; Doyle et al. 1989; Byrne et al. 1992; Bopp & Talcott 1978; Ramsey & Nation 1984; Strassmeier 1994). Indication of a systematic lag of 30–50° between plages and spots seems to emerge from the observations of these objects (Catalano et al. 1996, 2000a).

Rotational modulation of Ca II emission has been studied in several single main-sequence stars in the Mt. Wilson program (see e.g. Baliunas et al. 1985). Photometric monitoring of main-sequence stars with intermediate activity levels, i.e. stars similar to our Sun, has been pursued to study starspot activity (see e.g. Radick et al. 1983, 1998; Lockwood et al. 1997; Henry 1999). In particular, Radick et al. (1983) reported that two out of eleven stars monitored in *uvby* Strömgren pass-bands showed continuum light variation anti-correlated with the contemporaneous Ca II H+K *S* index. Lockwood et al. (1997) found low-amplitude variations in Strömgren *b* and *y* in about three quarters of the 41 program stars, monitored for about eleven years. They report photometric variability correlated with mean chromospheric activity, in the sense that the amplitude of the variation correlates with the mean chromospheric emission ratio $\log R'_{\rm HK}$. However, no study of contemporaneous photospheric and chromospheric short-term variability is included in that work. The most interesting work, in this respect, is that of Radick et al. (1998) where the photospheric and chromospheric behaviour of 35 stars, over a span of 11 years, is examined. These authors also studied the short-term variability behaviour (which is mainly due to rotational modulation) and, at least for 15 stars, they found a "negative" correlation (anti-correlation), with high statistical significance, between Strömgren photometry and Mt. Wilson Ca II H+K *S* measurements, indicative of spatial association of active areas at photospheric and chromospheric levels.

Send offprint requests to: A. Frasca (afr@sunct.ct.astro.it)

⋆ Based on observations collected at the Observatoire de Haute Provence (CNRS), France, and at the Osservatorio Astrofisico di Catania, Italy

Unfortunately, these authors do not present detailed light and *S* curves, as a function of the rotational phase.

Recent studies of the photospheric (by Doppler Imaging technique) and chromospheric inhomogeneities (by integrated line flux modulation) have analysed this topic more deeply, from high or moderate-resolution spectra (Strassmeier et al. 1993; Hatzes 1995; Neuhäuser et al. 1998; Stout-Batalha & Vogt 1999). All objects studied in these works are very young ultra-fast rotators (UFR) or pre-main sequence stars (PMS).

In particular, Strassmeier et al. (1993) found a marginal correlation between the starspots distribution and chromospheric inhomogeneities in LQ Hya (= HD 82558), a rapidly rotating ($P_{\rm rot} \simeq 1.6$ days) single K2 V star, probably just arriving on the ZAMS. However, they cannot conclusively decide whether plages or local chromospheric velocity fields cause the variations observed in the FWHM of the Hα line.

The two very active rapidly rotating Pleiades stars HII 686 and HII 3163, recently studied by Stout-Batalha & Vogt (1999), do not display maximum Hα and Ca II 8498 Å emission at the phase of spot transit.

Rotational modulation of the Hα emission with maximum nearly coincident with the minimum of the light curve has been detected by Frasca et al. (1997) in the active rapidly rotating binary TZ CrB (F6 V+G0 V, $P_{\rm orb} = 1\overset{\rm d}{.}14$).

In this paper we present the first photospheric/chromospheric study of HD 206860, a solar-type star with an activity level intermediate between the Sun and very active PMS and UFR stars, using, as chromospheric indicators, Ca II H & K and Hα lines. Simultaneous or nearly simultaneous photometric and spectroscopic observations have been performed.

HD 206860 (= HN Peg) is a young MS solar-type (G0 V) star which shows all signs of magnetic activity at photospheric, chromospheric and coronal level. In the framework of solar-stellar connection, HD 206860 represents a very stimulating case. Its activity has been recognized since the first spectroscopic surveys of Ca II H and K emission in cool stars (see e.g. Wilson 1968, 1978). Rotational modulation of emission was first reported by Stimets & Giles (1980) which found a period of $4\overset{\rm d}{.}69$ applying an autocorrelation technique to the Wilson (1978) data set. Subsequent analyses made on more extended data sets by Vaughan et al. (1981) and Baliunas et al. (1983, 1985) gave values of $4\overset{\rm d}{.}7$, $4\overset{\rm d}{.}63$ and $4\overset{\rm d}{.}67$, respectively. Donahue et al. (1996), from a periodogram analysis, found multiple periods within a single observing season, and different periods in different epochs ranging from a minimum of $4\overset{\rm d}{.}57$ to a maximum of $5\overset{\rm d}{.}30$. They ascribe such period variations to differential rotation coupled with changing latitude drift of active regions.

A strong coronal activity ($L_{\rm X} = 8 \times 10^{28}\,{\rm erg\,s^{-1}}$), nearly two orders of magnitude greater than the quiet Sun, but more than one order lower than the extremely active solar-type binaries TZ CrB and BI Cet, has been reported by Güdel et al. (1997).

Some indication of light variability was earlier reported by Blanco et al. (1979) who found, from UBV photometry, a periodicity of $24\overset{\rm d}{.}9$ (i.e. about 5 rotational periods) with an amplitude of $\sim 0\overset{\rm m}{.}02$ which seemed to be anti-correlated with the Mg II h and k lines. A smooth sinusoidal Δy light curve with an amplitude of 0.04 mag was presented by Reglero et al. (1986), folding their data with the rotational period $P_{\rm rot} = 4\overset{\rm d}{.}7$ given by Vaughan et al. (1981).

Values of the projected rotational velocity $v \sin i$ reported in the literature, though measured with different techniques, are fairly consistent between themselves. Kraft (1967), using a spectrocomparator, visually estimated $v \sin i = 11\,{\rm km\,s^{-1}}$, Soderblom (1982) from line profile fitting reported $10.2 \pm 1.1\,{\rm km\,s^{-1}}$, and Benz & Mayor (1984) from the width of the cross-correlation function measured $9.8 \pm 0.4\,{\rm km\,s^{-1}}$.

Table 1. Magnitudes and colors of the comparison (c), check (ck), and standard stars

HD	V	b–y	m_1	c_1
205852 (c)	5.450	0.203	0.170	0.892
206859 (ck)	4.340	0.709	0.468	0.354
207223	6.210	0.226	0.164	0.632
208565	5.560	0.036	0.148	1.126
208108	5.680	-0.010	0.182	1.005

2. Observations and data reduction

2.1. Photometry

The photometric observations have been carried out in the Strömgren *uvby* system with the 91-cm Cassegrain telescope at *M.G. Fracastoro* station (Serra La Nave, Mt. Etna) of Catania Astrophysical Observatory. The observations were performed with a photon-counting photometer equipped with an EMI 9893QA/350 photomultiplier, cooled to -15 °. We observed HD 206860 in 1998, July (7 nights) and August (3 nights) achieving a near complete coverage of the rotational period (4.74 days). HD 205852 ($V = 5\overset{\rm m}{.}45$, $B–V = 0\overset{\rm m}{.}30$) and HD 206859 ($V = 4\overset{\rm m}{.}34$, $B–V = 1\overset{\rm m}{.}17$) were used as comparison and check stars, respectively.

A set of *uvby* standard stars of known Strömgren indices (Lindemann & Hauck 1973) and V magnitude was nightly observed to transform the instrumental magnitudes of HD 206860 into the Strömgren photometric system. V magnitude and Strömgren photometric indices of the comparison and standard stars are given in Table 1.

The standard photometric sequence *sky-ck-c-v-c-sky* was repeated for about one hour each observing night. Normal points (one or two per night) were obtained by averaging groups of 4 individual measurements.

Table 2 shows the mean differential magnitudes (with respect to HD 205852). The average error in all filters is about 0.006 mag.

2.2. Spectroscopy

Simultaneous spectroscopic observations have been obtained in 1998 from June 17 to 28 at the *Observatoire de Haute Provence*

Table 2. Strömgren differential magnitudes of HD 206860, with respect to HD 205852.

Hel. Jul. Day −2400000	Δu (mag)	Δb (mag)	Δv (mag)	Δy (mag)
51010.53341	0.431	0.831	0.653	0.470
51011.53619	0.459	0.852	0.675	0.485
51011.54755	0.457	0.853	0.676	0.489
51012.54506	0.487	0.883	0.693	0.509
51012.55928	0.482	0.875	0.696	0.503
51013.53848	0.481	0.881	0.693	0.506
51013.55191	0.495	0.887	0.707	0.516
51014.54713	0.478	0.872	0.693	0.506
51014.55821	0.463	0.861	0.686	0.500
51022.53719	0.499	0.890	0.709	0.513
51022.54841	0.496	0.887	0.705	0.512
51024.47960	0.470	0.864	0.679	0.492
51082.39963	0.460	0.855	0.672	0.481
51082.40976	0.461	0.861	0.673	0.489
51083.43284	0.472	0.867	0.686	0.499
51086.39030	0.443	0.843	0.667	0.474

(OHP) and at the *M.G. Fracastoro* station of Catania Astrophysical Observatory.

At OHP we have observed HD 206860 in the Ca II H & K region within a program of survey of H & K profiles of F and G stars belonging to clusters and moving groups of different ages. The program has been performed by means of the AURELIE spectrograph connected to the coudé 152-cm telescope. The description and performance of the instrument are given in Gillet et al. (1994). Thanks to the very good weather conditions we had been continuously observing for all the 12 nights of the allocated time. In order to have a good definition of the H and K profiles and a wide portion of spectrum at the two sides of the two broad calcium lines, we selected grating No. 7 (1800 $lines/mm$) which yields a resolving power of 22 000 and a spectral band of about 140 Å, starting from λ 3880 Å. Due to the need of obtaining spectra of fainter stars for the survey program, we also used grating No. 3, which gives a resolving power of 7000, and a spectral band of 430 Å starting from λ 3830 Å. In total we have acquired 6 spectra at the higher resolution and other 6 at the lower one, as shown in Table 3.

Three additional spectra of HD 206860 were obtained with the ELODIE echelle spectrograph connected to the 193-cm telescope of OHP from July 2 to 5. The 67 orders recorded by the CCD detector cover the 3906-6818 Å wavelength range with a resolving power of about 42 000 (Baranne et al. 1996). They include the Ca II H & K lines in the first three orders, the Hα line in the 64$^{\rm th}$ order, the Li I 6708 Å line in the 67$^{\rm th}$ order, and a number of photospheric lines through all the optical spectrum.

The Hα observations carried out at Catania Observatory simultaneously with the AURELIE ones have been performed with the REOSC echelle spectrograph of the 91-cm telescope at *M.G. Fracastoro* station. We have used the spectrograph in the cross-dispersion configuration which gives a resolution of about 0.46 Å, as deduced from the FWHM of the Th–Ar calibration lamp. The spectrograph was fed by the telescope through an optical fiber (UV - NIR, $200\,\mu m$ core diameter) and was placed in a stable position in the room below the dome level. A front-illuminated CCD with 800×1152 pixels (pixel size of $22.5\,\mu m$) has been used. With this detector we could record four orders in each frame, spanning from about 6050 to 6650 Å, and nearly completely covering each echelle order. The signal-to-noise ratio (S/N) attained for HD 206860 was about 150.

Table 3. Log of the spectroscopic observations.

Date	UT_{midexp} h m	Instrument	R $\lambda/\Delta\lambda$	Wav. Range (Å)
June 17	25 30	AURELIE	22 000	3880–4020
" " 18	26 00	AURELIE	22 000	3880–4020
" " 19	26 00	AURELIE	22 000	3880–4020
" " 20	25 51	AURELIE	7000	3830–4260
" " 21	25 24	AURELIE	7000	3830–4260
" " 22	25 32	AURELIE	7000	3830–4260
" " 23	25 39	AURELIE	7000	3830–4260
" " 24	24 46	AURELIE	7000	3830–4260
" " 25	26 11	AURELIE	7000	3830–4020
" " 26	24 44	AURELIE	22 000	3880–4020
" " 27	25 29	AURELIE	22 000	3880–4020
" " 28	25 32	AURELIE	22 000	3880–4020
July 02	25 06	ELODIE	42 000	3906–6818
" " 04	26 10	ELODIE	42 000	3906–6818
" " 05	26 44	ELODIE	42 000	3906–6818
June 18	25 58	REOSC	14 000	6050–6650
" " 19	25 59	REOSC	14 000	6050–6650
" " 20	26 03	REOSC	14 000	6050–6650
" " 21	25 43	REOSC	14 000	6050–6650
" " 22	26 01	REOSC	14 000	6050–6650
" " 26	24 43	REOSC	14 000	6050–6650
" " 28	26 08	REOSC	14 000	6050–6650

In addition to the program stars, we observed several "inactive" stars of spectral type close or equal to that of HD 206860, to produce a reference Hα absorption profile needed for the spectral synthesis analysis. Actually, it is practically impossible to find G0 stars without any sign of magnetic activity, so we have chosen reference stars which are much less active than HD 206860, as shown by their low Ca II fluxes and/or by their faint Mg II h & k emission, for which we expect a negligible chromospheric contribution in the Hα core (Cayrel et al. 1983; Zarro & Rodgers 1983; Herbig 1985). The star which better mimics the Hα wings as well as the general appearance of the HD 206860 spectrum in the red region is 10 Tau (= HD 22484, F9 IV-V, B–V=0.58). Its very low activity degree is witnessed by the undetectable emission in the cores of the Ca II H & K lines (Strassmeier et al. 1990) as well as by the very faint emission in the Mg II h & K line cores that we have checked on IUE Final Archive spectra.

The reduction of AURELIE spectra was performed by the ONEDESPEC task of IRAF[1]. Since we are dealing with the very deep H and K lines, particular attention was paid to the back-

[1] IRAF is distributed by the National Optical Astronomy Observatory, which is operated by the Association of University for Research

ground subtraction. For this purpose we have used, for each night, all the offset and calibration lamp exposures in order to monitor and take into account the small fluctuations of the dark level typical of this instrument (Gillet et al. 1994).

We have also corrected our data for scattered light by means of Sun integrated-light spectra (the Moon and/or Jupiter satellites) and Arcturus spectra taken both at high and intermediate resolution. Since the H & K lines are very broad, their residual flux is largely independent of the spectral resolution for high or intermediate resolving powers (Gray 1992). The deepest part of the solar K-line profile has a 6–7% residual flux (Moore et al. 1966), while the K_1 points at the two sides of the central reversal in the Arcturus K-line deepen down to 5% (Gray 1992; Griffin 1968). We have normalized our solar spectra to the pseudo-continuum in agreement with the *Solar Spectrum* atlas (Moore et al. 1966), and the Arcturus spectra by taking the *Photometric Atlas of the Spectrum of Arcturus* (Griffin 1968) as reference. The Ca II K-line core of the solar spectrum we recorded with grating No. 7 has a minimum flux of 0.11, which indicates a 4% amount of scattered light. The K_1 residual flux of Arcturus spectrum is 0.08, again suggesting a 4% scattered light in such instrumental configuration. For the intermediate resolution spectra instead, we have derived a 9% scattered light level, after accounting for the small flattening of the lines ($\leq 1\%$) due to the lower resolution. The flattening has been evaluated by comparing the intermediate resolution spectra of the Moon and Arcturus with the high resolution spectra degraded to 0.58 Å.

The spectra have then been scaled to stellar surface flux taking as reference two spectral regions, at the two sides of the H & K lines, calibrated in star flux units using the Gunn & Stryker (1983) spectrophotometric atlas and the Barnes & Evans relationship (Barnes et al. 1978). The two continuous regions are centred on 3910 and 4010 Å and are 10 Å wide, as in the Gunn & Stryker spectrophotometry. Thus, we make the absolute flux calibration as much as possible independent of the spectral resolution.

The ELODIE spectra of HD 206860 are automatically reduced on-line during the observations. We have merged the first 4 spectral orders recorded by the detector to generate a spectral band suitable for the flux calibration, i.e. including the H & K lines and enough continuum at the two sides.

Fig. 1 shows 3 spectra in the Ca II H & K region taken at OHP with ELODIE and AURELIE, in high and intermediate resolution.

The echelle orders of ELODIE containing the Hα and the Li $\lambda\,6708$ line have been normalized to the local continuum, by a low-order (3 or 4) polynomial fit.

The reduction of Catania spectra was performed using the ECHELLE task of IRAF package, following the standard steps: background subtraction, division by a flat field spectrum given by a halogen lamp, wavelength calibration by means of the emission lines of a Thorium-Argon lamp, normalization through a polynomial fit to the continuum.

in Astronomy, inc. (AURA) under cooperative agreement with the National Science Foundation.

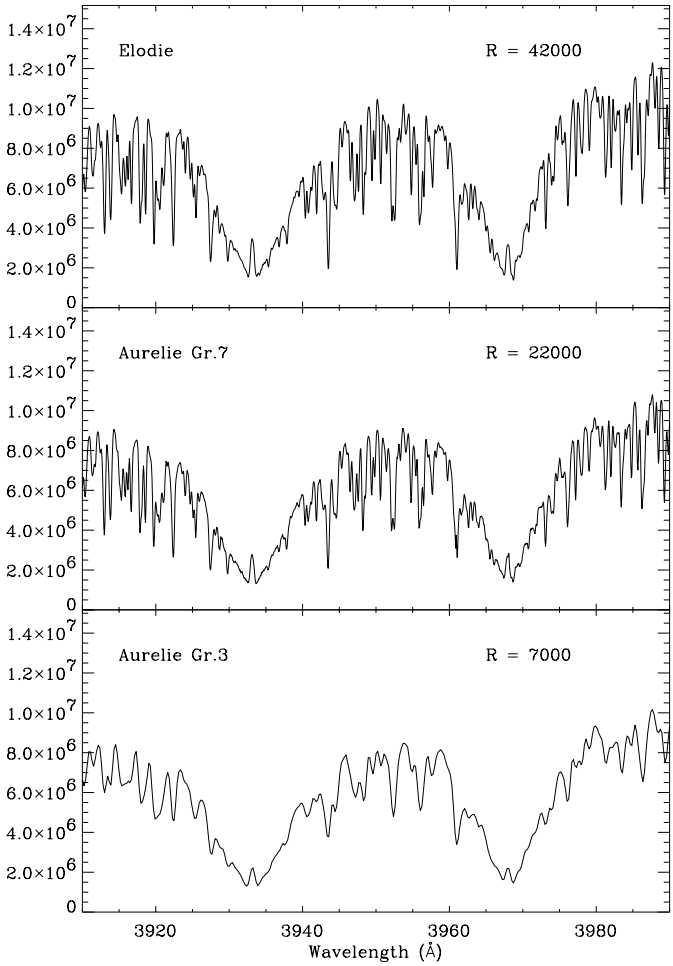

Fig. 1. Spectra in the Ca II H & K region taken at OHP with ELODIE and AURELIE in high and intermediate resolution.

The red part of the spectrum is contaminated by several telluric lines. We have removed the telluric water vapour lines at the Hα wavelengths using spectra of α Cep (A7 IV, $v\sin i = 240$ km s^{-1}) and Altair (A7 V, $v\sin i = 245$ km s^{-1}), which have a very broad and shallow Hα profile, acquired during the observing campaign. A fitting spline function, along all the spectrum (also inside the Hα profile), has been used to normalize these spectra and to provide valuable templates for the water vapour lines (see. Fig. 2).

An interactive procedure that allows the intensity of the template lines to vary (leaving unchanged the line ratios) until a satisfactory agreement with each observed spectrum is reached, has been applied to correct our HD 206860 spectra. A spectrum of HD 206860, before and after the telluric lines removal, is shown in Fig. 2 c,d as an example.

3. Data analysis and Results

3.1. Photometry

Since HD 206860 seems to display period variations in different observing seasons, presumably due to differential rotation (Donahue et al. 1996), we have performed a Fourier analysis

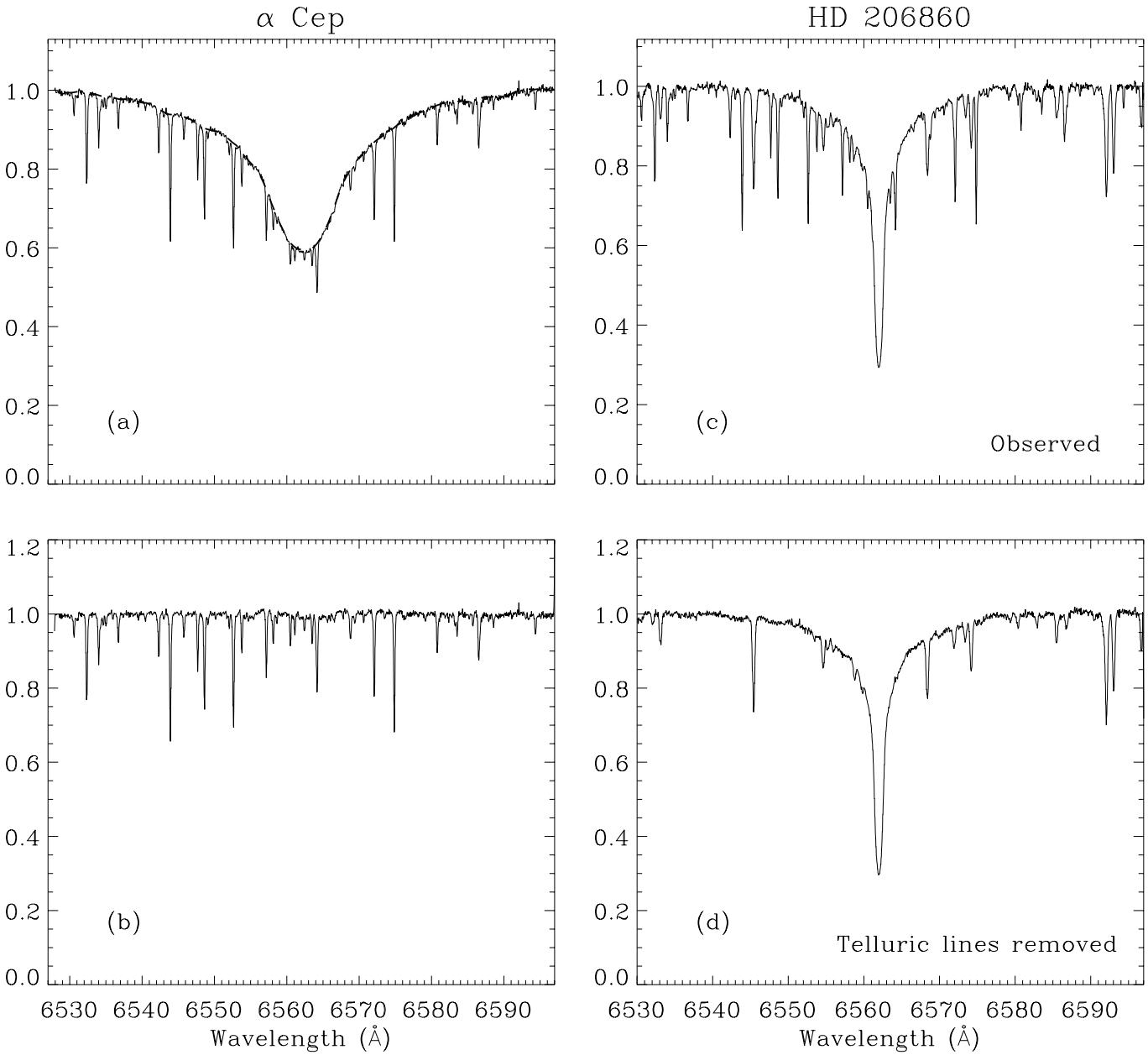

Fig. 2. **a** An ELODIE spectrum of the A7 IV rapidly rotating star α Cep, with the fit of the star spectrum (dotted line). **b** The "telluric template" obtained after division of the observed spectrum by the fit. An ELODIE spectrum of HD 206860 before (**c**) and after (**d**) the telluric lines removal, is also shown.

of our photometric time series with the aim of determining the average rotational period of the surface features seen in that observing season.

The Strömgren y photometry has been analysed by applying the Discrete Fourier Transform (DFT) technique. The CLEAN iterative deconvolution algorithm (Roberts et al. 1986) has been used to eliminate the effects of the observation spectral window in the power spectrum.

The cleaned periodogram for the Δy data set is displayed in Fig. 3. A sharp peak corresponding to a period of $4\overset{\mathrm{d}}{.}74 \pm 0\overset{\mathrm{d}}{.}12$ is apparent. The error has been estimated from the half-width at half-maximum of the peak in the cleaned periodogram. Taking into account the error, this period is compatible with the values reported by Stimets & Giles (1980), Vaughan et al. (1981), Baliunas et al. (1983, 1985). This value is also a rough average of the rotational periods found by Donahue et al. (1996). We have used our period to fold in phase both the photometric and spectroscopic data for the subsequent analysis.

Fig. 4 shows the Δy light curve and the three Strömgren color curves *b-y*, *v-y*, *u-y*. The *u-v* color is also shown on the top of Fig. 4. The photometric light curve in the y filter shows a fairly peaked maximum and rather a flat minimum. The variation amplitude $\simeq 0\overset{\mathrm{m}}{.}035$ is comparable with the amplitude found by Reglero et al. (1986), also the shape of the light curve is very

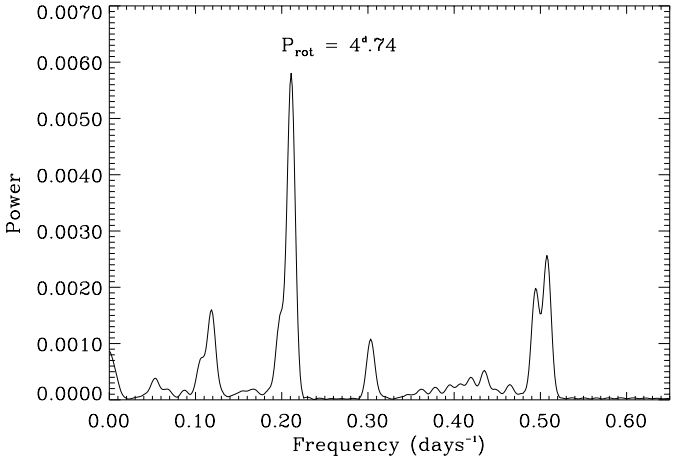

Fig. 3. Cleaned periodogram for our Δy photometry of HD 206860.

similar. The color curves show low amplitude variations that are correlated with the light curve, i.e. the star is redder when it is at light minimum. In addition, the amplitude of the color variation increases with the effective wavelength difference of the filters, $u-y$ showing the largest variation. We did not find any rotational modulation (within $0\overset{\mathrm{m}}{.}01$) of the metallicity index m_1, therefore we can rule out the possibility that the differential effect of metallicity is responsible for the in-phase variations of the $v-y$ and $u-y$ color indices. So, the observed color variation behaviour is in agreement with the hypothesis that luminosity variation has its origin in cool starspots.

In some very active stars, notably UX Ari, HR 1099, and HK Lac, an anti-correlation between the Johnson U–B color index and the V light curve has been observed during the periods of stronger activity (Catalano et al. 1996, 2000a) thus suggesting that plages are prominent in the near-UV continuum. We do not see this effect in the HD 206860 ultraviolet color $\Delta(u-y)$, the most sensitive to facular contribution, so that it seems that the plages manifest themselves only in the chromospheric lines, but do not appreciably contribute to the near-UV continuum.

The average V magnitude and Strömgren indices have been also calculated using Olsen's (1983) method. We have transformed the observed instrumental magnitude y_0 and color indices using transformation coefficients based on comparison and standard stars given in Table 1. The estimated values with their errors are $V = 5.962 \pm 0.017$, $b-y = 0.380 \pm 0.009$, $m_1 = 0.166 \pm 0.010$, and $c_1 = 0.307 \pm 0.017$, in good agreement with previous determinations (Fabregat & Reglero 1990; Olsen 1994).

3.2. Lithium abundance

The strong lithium λ6708 line displayed in the ELODIE spectra is indicative of the young age of HD 206860 (see e.g. Soderblom 1983).

The equivalent width of the lithium λ6708 line (0.106 ± 0.005 Å) was measured on three ELODIE spectra (see Fig. 5). The quoted error is the weighted average of the individual errors on each EW measurement, which we derive as the

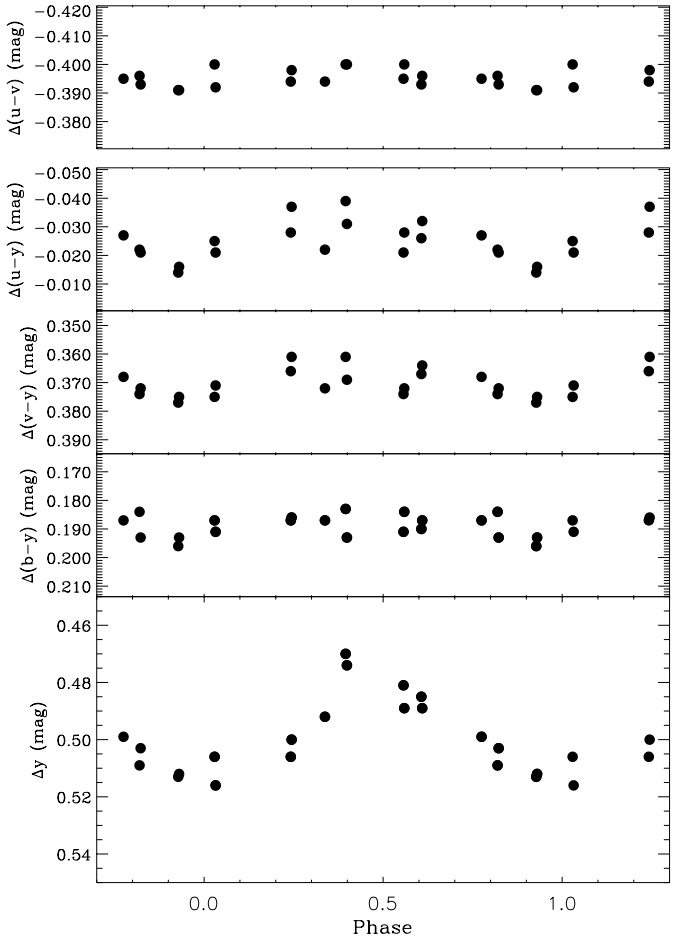

Fig. 4. Strömgren Δy and color curves of HD 206860.

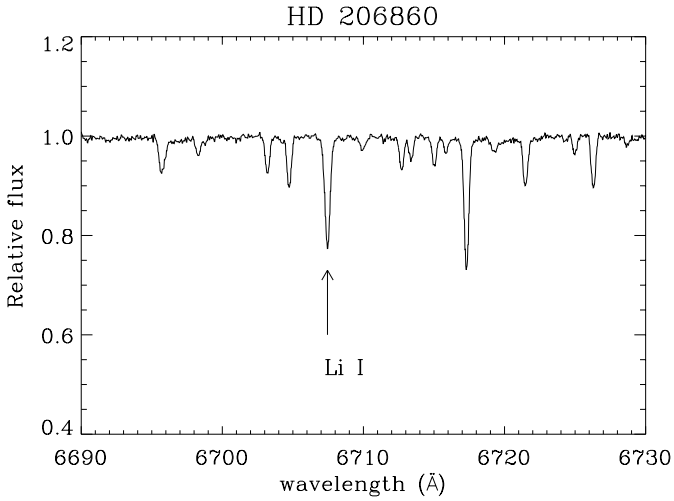

Fig. 5. The Li I λ 6708 Åřegion of HD 206860 as recorded with ELODIE.

product of the integration range to the $(S/N)^{-1}$ ratio, evaluated in two line-free windows selected at the two sides of the Li I line. The error value we obtained is typical of high-resolution, high signal-to-noise spectra (Soderblom 1990). The average EW of the Li I line has been corrected for the small contribution of a

near Fe I line ($\lambda\,6707.4$ Å) according to the empirical relation found by Soderblom et al. (1993). The average corrected value EW_{Li} = 0.097 Å leads to a Li abundance $N(\mathrm{Li}) = 2.9 \pm 0.1$, according to Pavlenko & Magazzù (1996) NLTE calculation, when an uncertainty of one spectral type subclass is also considered. This value results to be higher than the value 2.65 reported by Duncan (1981), and is slightly different from $N(\mathrm{Li}) = 3.08$ reported by Gaidos (1998). Our value is also significantly lower than the undepleted cosmic lithium abundance $N(\mathrm{Li}) = 3.2$. As remarked by the works of Soderblom et al. (1993) and Jefferies (1995), Li abundance for early G stars (B–V $\leq$ 0.6) is not a good age indicator, at least till the Hyades age (600 Myr), due to the low rate of lithium depletion for this mass. Nevertheless, the lithium content of HD 206860 seems to be a bit lower than that typical of early G-type Pleiades stars and more consistent with that of the UMa stream stars (300 Myr) or slightly older.

A better estimate of the age can be derived from *rotation–age* or *activity–age* relationships. From *activity–age* and P_{rot}*–age* relations, Soderblom (1983) derived an age of about 400 and 200 Myr, respectively. From our own calibrations of Ca II H & K luminosity versus age (Catalano et al. 2000b), we found an age of 280 Myr for HD 206860.

Furthermore, the space velocity of this star, re-determined by Gaidos (1998) by means of Hipparcos parallax and proper motion, seems to indicate that HD 206860 belongs to the so-called Local Association (or Pleiades Group), a moving group composed of young stars with average components of space velocity $U, V, W = -11, -21, -11$ (Eggen 1992; Jefferies 1995), whose members are 100–300 Myr old.

3.3. *Ca* II *integrated flux*

We have measured the chromospheric flux in the cores of the Ca II lines with a procedure which allows us to define the photospheric profile inside the line core. This method enables us to better define the chromospheric emission contribution and to minimize any residual difference in the scattered light or bias correction. We have simulated an inactive profile of H & K lines as the sum of a Lorentzian which fits the wings of the absorption Ca II lines and a Gaussian that mimics, in the line cores, the shape of a synthesized spectrum in radiative equilibrium (see Catalano et al. 2000b). We used this simulated photospheric profile because we are mainly interested in the line core variation rather than into an accurate modelling of the Ca II lines. However, apart from a time-consuming work to perform accurate R.E. modelling which is out of the present analysis scope, a direct integration between the K_1 and H_1 points, also taking into account the radiative equilibrium contribution in the line core, as evaluated by Linsky et al. (1979), gives rise to an average value of the flux $F_{\mathrm{H_1+K_1}} \simeq 4.7 \times 10^6 \mathrm{erg\,cm^{-2}s^{-1}}$ with much more scatter and a negligible evidence of rotational modulation.

The advantage of our method is a better definition of the core emission against a reasonable "non-active" profile. The slight mismatch in the outer wings, heavily affected by many absorption lines, has no effect on the emission flux measurement which is obtained integrating the inner part of the line. The fit of such profile has been performed (separately for the H and K lines) for one high resolution AURELIE spectrum. This template profile has been subtracted from each spectrum, after the application, whenever necessary, of a flux shift to fit the inner wing level of the absorption profile. This residual offset between different spectra (always less than 0.5%) is presumably due to slight differences in the continuum level evaluation by the polynomial fitting. An example of the application of this technique is shown in Fig. 6. The subtraction of the simulated profile leaves a pure emission in the line core that can be integrated to evaluate the chromospheric line flux.

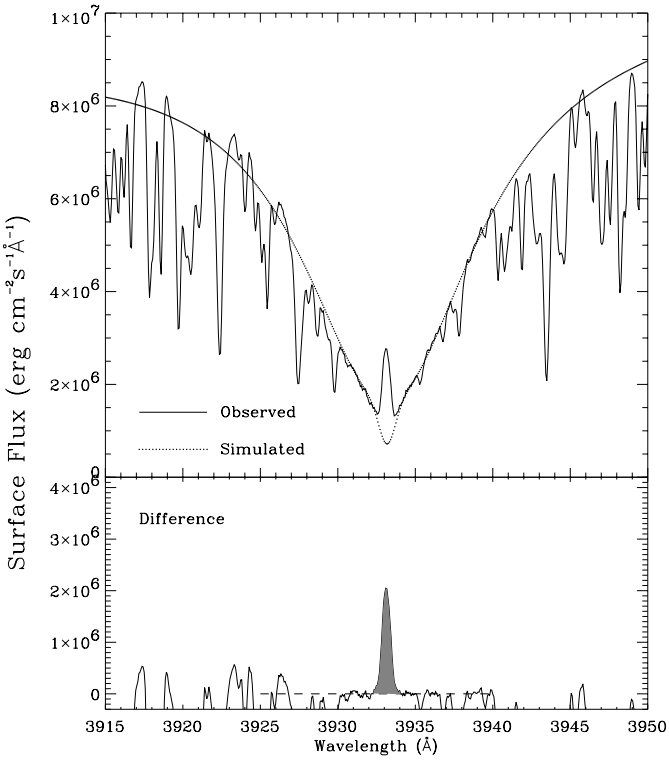

Fig. 6. An example of the subtraction technique applied to the K line of an AURELIE spectrum of HD 206860. A simulated profile is shown in dotted line. In the bottom panel the result of the subtraction is shown.

Since the simulated absorption profile has been derived from an AURELIE spectrum, the ELODIE merged Ca II spectra have been degraded in resolution from 42 000 to 22 000, by convolving the original spectra with a Gaussian kernel of the appropriate FWHM, before the flux measurements. Thus, these spectra, though with more pixels per resolution element, have been made homogeneous with the other grating-7 AURELIE spectra, improving in the meanwhile their signal-to-noise ratio.

In order to apply the method to the spectra obtained with grating No. 3 of AURELIE, the simulated profile has been degraded to the resolution $\lambda/\Delta\lambda = 7000$. The effect of the lower resolution on the narrow emission peak in the line centers is a slight reduction in the peak intensity, i.e. in the contrast, and, as a consequence, a lower sensitivity to variations. In order to safely use low and high resolution data, we have evaluated the reduction factor in the integrated fluxes when the high resolu-

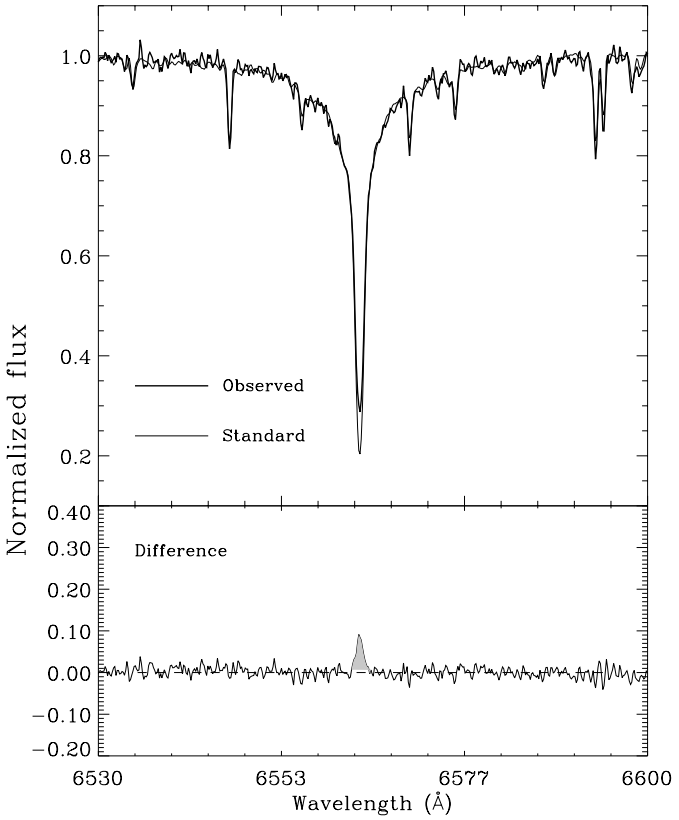

Fig. 7. An Hα profile of HD 206860 (solid line) with the superimposed rotationally broadened spectrum of the standard star 10 Tau (dotted line). The Hα core emission is evident in the difference spectrum (filled area).

tion spectra are degraded to 0.58 Å. On average, we found a factor of 0.8. Then the line flux values coming from the lower resolution spectra have been divided by this factor before being compared with the others.

We have estimated the errors in the integrated fluxes as the product of the photometric error on each spectral point, given by the reciprocal of the S/N at the bottom of the line, by the integration range. The relative values are reported as error bars in Fig. 8. These chromospheric Ca II absolute fluxes and relative errors are listed in Table 4.

3.4. Hα chromospheric filling

To simulate HD 206860 Hα spectrum as it would be in absence of a strong chromospheric emission we have used a high S/N spectrum of 10 Tau acquired at Catania Observatory and rotationally broadened to the $v \sin i = 10\,\mathrm{km\,s^{-1}}$ of HD 206860.

In Fig. 7 a spectrum of HD 206860 in the Hα region obtained at Catania Observatory is shown with a thick line together with the "inactive template" (thin line), built up as described before. In the difference spectrum a significant positive peak above the noise is clearly seen.

The three ELODIE spectra have been used degrading the echelle order containing the Hα line to the spectral resolution of Catania spectra ($R = 14\,000$). Then the subtraction of the inactive template, built up with the spectrum of 10 Tau obtained at Catania Observatory, has been performed to isolate the Hα chromospheric emission core. The net Hα equivalent width, $EW_{\mathrm{H}\alpha}$, has been measured in such "difference" spectra by integrating the net emission profile (grey area in Fig. 7). The $EW_{\mathrm{H}\alpha}$ values together with the relative errors are listed in Table 5.

Our $EW_{\mathrm{H}\alpha}$ values are in the range 0.108–0.156 Å, so that the minimum value is comparable, but a bit larger (about 20%), with the value 0.09 Å reported by Herbig (1985), who used β CVn as reference star. This discrepancy can be due to the use of different standard stars (β CVn is indeed a bit more active than 10 Tau, as witnessed by its emission in the core of Mg II h and k lines), as well as to a lower degree of activity of HD 206860 at the time of Herbig's observations.

Table 4. Chromospheric Ca II fluxes.

Hel. Jul. Day −2400000	Ca II H+K flux (10^6 erg cm^{-2}s^{-1})	error	Instrument
50982.56454	3.08	0.21	AURELIE G. 7
50983.58535	3.35	0.62	" "
50984.58573	3.57	0.30	" "
50991.53302	3.44	0.76	" "
50992.56482	3.21	0.24	" "
50993.56647	3.55	0.30	" "
50985.57944	2.66	0.12	AURELIE G. 3
50986.56083	2.59	0.17	" "
50987.56656	2.63	0.16	" "
50988.57114	2.73	0.16	" "
50989.53435	3.11	0.22	" "
50990.59392	2.92	0.68	" "
50997.54928	3.24	0.22	ELODIE
50999.59325	3.61	0.23	" "
51000.61749	3.49	0.12	" "

Table 5. Hα EW.

Hel. Jul. Day −2400000	$EW_{\mathrm{H}\alpha}$ (Å)	error (Å)	Instrument
50997.54928	0.127	0.010	ELODIE
50999.59325	0.155	0.018	" "
51000.61749	0.119	0.014	" "
50983.58400	0.124	0.024	REOSC
50984.58460	0.156	0.027	" "
50985.58786	0.128	0.027	" "
50986.57353	0.112	0.021	" "
50987.58640	0.108	0.019	" "
50991.53253	0.110	0.021	" "
50993.59172	0.133	0.019	" "

4. Rotational modulation

Chromospheric emission flux in the Ca II and in the Hα lines has been obtained with the aim of detecting rotational modulation induced by an uneven distribution of active regions.

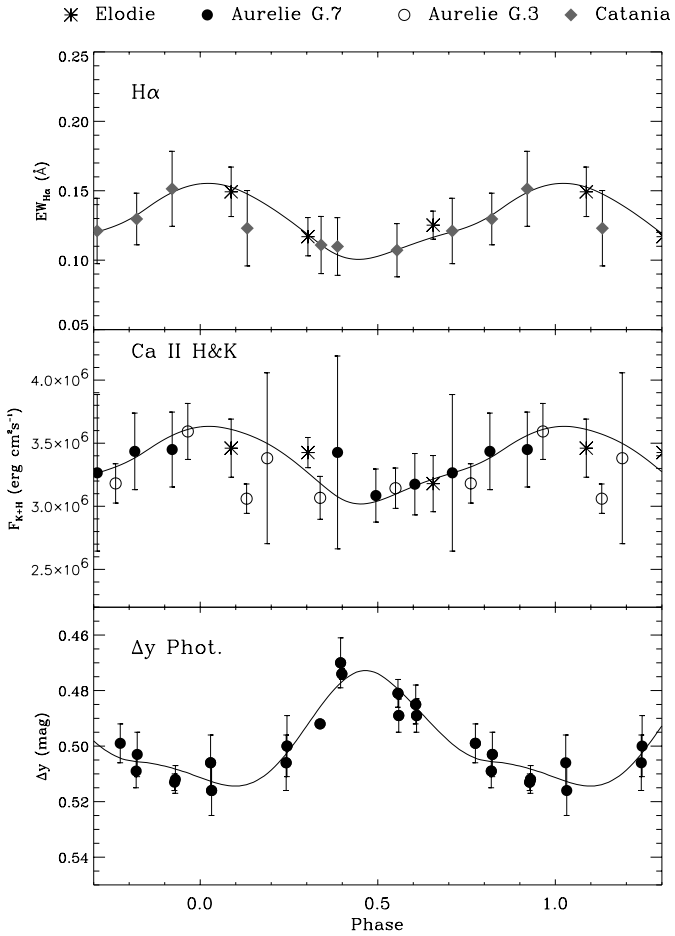

Fig. 8. Net Hα EW, Ca II H+K surface flux and Strömgren Δy photometry displayed as a function of the rotational phase. The continuous lines superimposed on the points in each box represent the plage/spot solutions.

The difference between the spectra and the simulated profile has been integrated along the residual emission profile to yield the chromospheric emission flux (Figs. 6 and 7). The Ca II fluxes are given in absolute units at stellar surface, while Hα fluxes are given as equivalent widths. Both the excess emission in the Ca II H and K lines and in the Hα show asymmetric variations with very similar behaviour and amplitude of 20% and 40%, respectively.

Since the Hα emission EW and the Ca II core flux are measured against the local continuum, the time variation of the latter, seen from the photometry, would induce "anti-correlated" EW emission variations even if the real emission is constant. To evaluate the "true" Hα EW and Ca II fluxes, an unspotted reference continuum level must be defined. The "observed" $EW_{\rm H\alpha}$ and Ca II fluxes have been corrected by the effect of the continuum variation, i.e. each $EW_{\rm H\alpha}$ and $F_{\rm CaII\,H+K}$ value has been scaled to the continuum maximum light (presumed unspotted level) adopting the modelled light curves (see next section) in the Strömgren *y* and *v* pass-bands (for Hα and Ca II, respectively). The maximum correction amounts to about 4%, leading to variation amplitudes of 16% and 36% for the Ca II and the Hα respectively.

The Hα and Ca II line-fluxes, together with the Δy photometry, are displayed in Fig. 8 as a function of the rotational phase reckoned from the ephemeris $\mathrm{HJD}_0 = 2450966.0 + 4\overset{\mathrm{d}}{.}74 \times E$, where the initial epoch (June 1st at noon) has been arbitrarily chosen.

Both the Ca II and Hα chromospheric flux curves, apart from the scatter, display a regular trend with the rotational phase and appear anti-correlated with the photospheric light curve. This implies a good spatial correlation between the starspots and the chromospheric plages as seen at the Hα and Ca II levels.

In order to better establish the degree of modulation with the phase of the three diagnostics, we have calculated the Spearman's rank correlation coefficients of Δy, $EW_{\rm H\alpha}$ and $F_{\rm CaII\,H+K}$ values with a simple cosine function ($\cos 2\pi\phi$), by means of the IDL procedure for rank-correlation analysis R_CORRELATE (Press et al. 1986). The "two-sided significance" of their deviation from zero has been also calculated. The correlation coefficients are $\rho_{\Delta y} = -0.894$, $\rho_{H\alpha} = 0.915$, and $\rho_{\rm CaII} = 0.771$, with significance $3{\times}10^{-6}$, $2{\times}10^{-4}$, $8{\times}10^{-4}$, respectively. This means that in all cases there is a very good, or at least acceptable (as in the Ca II case) correlation of variations with the rotational phase.

We have also tested the anti-correlation between the photometry and Hα EW and Ca II flux as functions of the rotational phase. We have found a correlation coefficient ρ = -0.905 with a significance 0.0014 for the correlation Δy–Hα, and ρ = -0.767 with significance 0.016 for Δy–$F_{\rm CaII\,H+K}$. This test indicates rather a high degree of anti-correlation between continuum light and chromospheric line-flux variation.

In order to further investigate the spatial association between photospheric and chromospheric active regions and to give a rough reconstruction of the surface inhomogeneities we have applied a spot/plage model to the corrected flux curves.

A key parameter needed for the application of a spot model is the inclination i of the rotational axis with respect to the line of sight. A reasonable estimate of i for a single star is obtained from $v \sin i$ and the rotational period $P_{\rm rot}$.

The projected rotational velocity can be written

$$v \sin i = 2\pi R \sin i / P_{\rm rot} = 10\,\mathrm{km\,s^{-1}} \quad (1)$$

where $10\,\mathrm{km\,s^{-1}}$ is the mean of the values reported by Soderblom (1982) and by Benz & Mayor (1984). Assuming a radius $R = 1.08\,R_\odot$, typical of a G0 V star (see e.g. Gray 1992) with an uncertainty of 0.04 $R_\odot$ corresponding to a spectral type subclass uncertainty, we derive an inclination $i = 62^\circ \pm 8^\circ$ from Eq. 1. The error on i has been evaluated taking into account the period uncertainty (2.5%), the uncertainty on the radius (3.7%) and the error on the rotational velocity $v \sin i$ which is of $\simeq 0.5\,\mathrm{km\,s^{-1}}$ (i.e. 5%) for both measurements.

From the Δy light curve the usual parameters of dark spots $\{\mathrm{T_s/T_*}$, $\mathrm{R_s}$, lon, lat$\}$ have been searched for using the Binary Maker (Bradstreet 1993) interactive program. The temperature ratio between the spots and the surrounding photosphere $\mathrm{T_s/T_*}$ has been kept constant to 0.75, a typical value of sunspot umbrae.

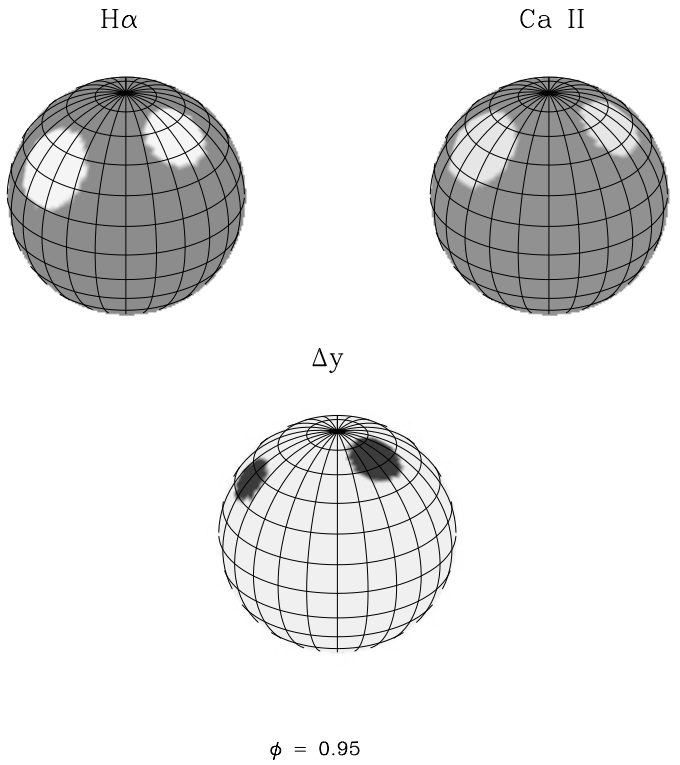

Fig. 9. Schematic representations of the chromosphere (at Ca II and Hα levels) and photosphere of HD 206860 as reconstructed by the adopted plage and spot models. In these snapshots the star is seen at phase 0.95 and is rotating counterclockwise.

For the Hα and Ca II plages we have performed solutions with bright spots. Flux ratios F_{plage}/F_{chrom} between the plage and quiet chromosphere typical of the maximum solar plage values, i.e. 5 and 3 for Hα and Ca II lines, respectively, have been adopted (see e.g. Ayres et al. 1986).

Solution have been independently sought for the three diagnostics with the assumption that plages have equal radii in both chromospheric indicators. We have interactively searched for the best solution varying the radii, longitudes and latitudes of the active regions. This allows us to look for "geometrical solutions" where the size of the "bright spots" is only indicative and is not completely independent of the flux ratio assumed. Nevertheless, the product of the plage area by the flux contrast can be taken as a good indicator of the facular activity contribution. Obviously, the most accurate parameter is the spot/plage longitude, the latitudes and the sizes being only first order approximate values. Due to the asymmetric shape of the curves, all the solutions required two active areas.

In order to test the significance of our fits to the data, we have calculated the r.m.s. around the solutions and compared it to the intrinsic scatter of the data themselves (their standard deviation). We found that the r.m.s. is noticeably reduced, by a factor $\approx$2–3, after subtraction of the fitting curves for $EW_{\rm H\alpha}$ and Δy. A 30% lower r.m.s. is found for $F_{\rm CaII\,H+K}$, applying a 3σ confidence threshold criterion to the data. These results are consistent with the rank-correlation analysis.

The parameters of the model solutions are listed in Table 6. A schematic drawing of the photospheric and chromospheric inhomogeneities is shown in Fig. 9. As can be seen from Table 6, there is a good coincidence between the position of spots and plages. Anyway, spot #2 seems to follow plage #2, at both Hα and Ca II level, by about 20° in longitude. A similar longitude difference between spot #1 and plage #1 takes place for Ca II, but not for Hα. However, due to the scatter of chromospheric data and the high latitude of these surface features, the precision on the plage longitude that we can attain (estimated as $\approx 15-20°$, corresponding to a fraction of orbital period of about $^{\rm p}.05$) is comparable with the longitudinal separation between spot and plages derived from the spot/plage model. Therefore we conclude that spots and plages coincide within the errors and the 20° longitude difference between spot #2 and plage #2 is marginally significant.

The interpretation of stellar data is necessarily guided by solar analogy. In this framework, it is instructive to recall that the studies of Brown & Evans (1980) and Chapman et al. (1997) on the behaviour of facular to sunspot areas along the activity cycle have shown, as a general picture, that spots lead plages by few degrees. In particular Dobson-Hockey & Radick (1986) show that sunspots lead the associated plages by an amount that is proportional to the plage area.

Moreover, Catalano et al. (1998), correlating the irradiance measurements of integrated Sun in the C II chromospheric line (λ 133.5 nm), from UARS SOLSTICE experiment (Rottman et al. 1993), with the sunspot number, have found that the times of C II emission and spot number maxima at each rotation alternate positive and negative differences in a periodic fashion. The estimated period is about 270 days and the maximum difference 5 days. The average position of spots thus appears to precede or follow the centroid of plages by about $30-40°$, in a period of about 10 solar rotations, i.e. in a time comparable to the faculae lifetime.

Although spots and plages seem to follow a solar-like behaviour in some respect, the presence of a high-latitude spot seems to indicate a non-solar situation, more typical of very active stars. HD 206860 does not appear to follow the typical solar case as observed on detailed disk observations (Brown & Evans 1980; Chapman et al. 1997; Dobson-Hockey & Radick 1986), but could be assimilated into a particular situation with plages leading spots seen on the Sun as a star (Catalano et al. 1998).

5. Conclusions

The analysis of quasi-contemporaneous observations, both spectroscopic and photometric, of HD 206860 has given remarkable results in the study of the connection between photospheric and chromospheric activity in a single young active star of solar type.

HD 206860 displays a clear rotational modulation in all the chromospheric and photospheric indicators (Ca II, Hα, Δy), thus confirming previous observations (Stimets & Gilets 1980; Baliunas et al. 1983, 1985; Fabregat & Reglero 1990) and indi-

Table 6. Spots and plages parameters

Diags.	Feature	Radius	Lon.[a]	Lat.	$\frac{F_{plage}}{F_{chr}}$	$\frac{T_{spot}}{T_{phot}}$
Hα	# 1	$16\overset{\circ}{.}5$	295°	55°	5	
	# 2	$20\overset{\circ}{.}5$	34°	35°	5	
Ca II	# 1	$16\overset{\circ}{.}5$	275°	55°	3	
	# 2	$20\overset{\circ}{.}5$	40°	45°	3	
Δy	# 1	$13\overset{\circ}{.}5$	293°	65°		0.75
	# 2	$11\overset{\circ}{.}5$	58°	40°		0.75

[a] Longitude increases with phase, and 0° longitude corresponds to phase $0\overset{p}{.}0$.

cating the presence of uneven distribution of long-lived active regions.

A nice correlation between Ca II H+K and Hα emission fluxes implying a good spatial association between chromospheric plages at two different atmospheric levels has been found. In spite of the small line core filling-in, the net Hα equivalent width shows a higher modulation amplitude than the Ca II flux. This is indicative of a contrast of the Hα plages (compared to the surrounding chromosphere) stronger than that of the Ca II plages, in agreement with previous findings on the Sun (Ayres et al. 1986).

Finally, from a simple model analysis, spatial association between photospheric spots and chromospheric plages, as found in the Sun and in the most active RS CVn systems (Catalano et al. 2000a), has been pointed out. We have also found a possible indication that spots in HD 206860 tend to follow plages by about 20°. This does not appear to be a typical solar case as seen in disc resolved observations where generally spots lead plages (Brown & Evans 1980; Chapman et al. 1997; Dobson-Hockey & Radick 1986). Since our analysis, obviously, represents a snapshot of the active region configuration of HD 206860, more repeated observations are required to study any time dependence, as seen on the Sun observed as a star (Catalano et al. 1998).

In order to settle this issue we should have more data. With this aim we are carrying out simultaneous photometric and spectroscopic observations of other single solar-type stars to investigate possible systematic longitude differences as a function of stellar parameters, and rotational rates, i.e. of the dynamo action.

However, both photometric and spectroscopic observations with very high resolution, and the use of inversion techniques (like Doppler Imaging) which give more reliable information also on latitudes are strongly desirable.

Acknowledgements. This work has been supported by the Italian *Ministero dell' Università e della Ricerca Scientifica e Tecnologica*, the *Gruppo Nazionale di Astronomia* of the CNR and by the *Regione Sicilia* which are gratefully acknowledged. We would like to thank the valuable support of the technical staff of Catania and Haute Provence Observatories. We would like to thank the referee, Klaus G. Strassmeier, for several helpful comments. This research has made use of the SIMBAD database, operated at CDS, Strasbourg, France, and of the General Catalogue of Photometric Data (GCPD) operated at the University of Lausanne, Switzerland.

References

Ayres T.R., Testerman L., Brault J.W., 1986, ApJ 304, 542
Baliunas S.L., Vaughan A.H., Hartmann L., et al., 1983, ApJ 275, 752
Baliunas S.L., Horne J.H., Porter A., et al., 1985, ApJ 294, 310
Baranne A., Queloz D., Mayor M., et al., 1996, A&AS 119, 373
Barnes T.G., Evans D.S., Moffet T.J., 1978, MNRAS 183, 285
Benz W., Mayor M., 1984, A&A 138, 183
Blanco C., Marilli E., Catalano S., 1979, A&AS 36, 297
Bopp B.W., Talcott J.C., 1978, AJ 83, 1517
Bradstreet D.H., 1993, Binary Maker 2.0 User Manual, Contact Software
Brown G.M., Evans D.R., 1980, Solar Phys. 66, 233
Byrne P.B., Agnew D.J., Cutispoto G., et al., 1992, In: Byrne P.B., Mullan D.J. (eds.) Surface Inhomogeneities on Late-Type Stars. Springer Verlag, Berlin, p. 255
Catalano S., Rodonò M., Frasca A., Cutispoto G., 1996, In: Strassmeier K.G., Linsky J. (eds.) Stellar Surface Structure. IAU Symp. No. 176, p. 403
Catalano S., Lanza A.F., Brekke P., Rottmann G.J., Hoyng P., 1998, In: Donahue R.A., Bookbinder J.A. (eds.) The 10th Cambridge Workshop on Cool Stars, Stellar Systems and the Sun. ASP Conf. Ser. vol. 154, p. 584
Catalano S., Rodonò M., Cutispoto G., et al., 2000a, In: İbanoğlu C. (ed.) Variable Stars as Essential Astrophysical Tools. Kluwer Academic Publishers, p. 687
Catalano S., Frasca A., Marilli E., Freire Ferrero R., Trigilio C., 2000b, In: Pallavicini R. (ed.) Stellar Clusters and Associations: Convection, Rotation, and Dynamos. ASP Conf. Ser. vol. 198, p. 439
Cayrel R., Cayrel de Strobel G., Campbell B., et al., 1983, A&A 123, 89
Chapman G.A., Cookson A.M., Dobias J.J., 1997, ApJ 482, 541
Donahue R.A., Saar S.H., Baliunas S.L., 1996, ApJ 466, 384
Dobson-Hockey A.K., Radick R.R., 1986, In: Zeilik M., Gibson D.M. (eds.) Cool Stars, Stellar Systems and the Sun. 4th Cambridge Cool Star Workshop, Springer-Verlag, Berlin, p. 202
Doyle J.G., Byrne P.B., Van den Oord G.H.J., 1989, A&A 224, 153
Duncan D.K., 1981, ApJ 248, 651
Eggen O.J., 1992, AJ 103, 1302
Fabregat J., Reglero V., 1990, A&AS 82, 531
Frasca A., Catalano S., Mantovani D., 1997, A&A 320, 101
Frasca A., Catalano S., Marilli E., 1998, In: Bookbinder J.A., Donahue R.A. (eds.) The 10th Cambridge Workshop on Cool Stars, Stellar Systems and the Sun. ASP Conf. Ser. vol. 154, p. 1521
Gaidos E.J., 1998, PASP 110, 1259
Gillet D., Burnage R., Kohler D., et al., 1994, A&AS 108, 181
Gray D., 1992, The Observation and Analysis of Stellar Photospheres. Second edition, Cambridge University Press, p. 260
Griffin R.F., 1968, A Photometric Atlas of the Spectrum of Arcturus. Cambridge Philosophical Soc., Cambridge
Güdel M., Guinan E.F., Skinner S.L., 1997, ApJ 483, 947
Gunn J., Stryker L.L., 1983, ApJS 52, 121
Hatzes A.P., 1995, ApJ 451, 784
Henry G.W., 1999, PASP 111, 845
Herbig G.H., 1985, ApJ 289, 269
Jefferies R.D., 1995, MNRAS 273, 559
Kraft R.P., 1967, ApJ 150, 551
Lindemann E., Hauck B., 1973, A&AS 11, 119
Linsky J.L., Worden S.P., McClintock W., Robertson R.M., 1979, ApJS 41, 47
Lockwood G.W., Skiff B.A., Radick R.R., 1997, ApJ 485, 789

Moore C.E., Minnaert M.G.J., Houtgast J., 1966, The Solar Spectrum 2935 Å to 8770 Å. National Bureau of Standards, Washington, Monograph 61
Neuhäuser R., Wolk S.J., Torres G., et al., 1998, A&A 334, 873
Olsen E.H., 1983, A&AS 54, 55
Olsen E.H., 1994, A&AS 106, 257
Pavlenko Y.V., Magazzù A., 1996, A&A 311, 961
Press W.H., Flannery B.P., Teukolsky S.A., Vetterling W.T., 1986, Numerical Recipes. The Art of Scientific Computing. Cambridge University Press
Priest E.R., 1982, Solar Magneto-Hydrodynamics. D.Reidel Publ. Co., Dordrecht, Holland
Radick R.R., Wilkerson M.S., Worden S.P., et al., 1983, PASP 95, 300
Radick R.R., Lockwood G.W., Skiff B.A., Baliunas S.L., 1998, ApJS 118, 239
Ramsey L.W., Nation H.L., 1984, AJ 89, 115
Reglero V., Fabregat J., De Castro A., 1986, Inf. Bull. Var. Stars. 2904
Roberts D.H., Lehár J., Dreher J.W., 1986, AJ 93, 968
Rodonò M., Byrne P.B., Neff J.E., et al., 1987, A&A 176, 267
Rottman G.J., Woods T.N., Sparn T.P., 1993, Journal Geophys. Res. 98, 10667
Soderblom D.R., 1982, ApJ 263, 239
Soderblom D.R., 1983, ApJS 53, 1
Soderblom D.R., 1990, AJ 99, 595
Soderblom D.R., Jones B.F., Balachandran S., et al., 1993, AJ 106, 1059
Stimets R.W., Giles R.H., 1980, ApJ 242, L37
Stout-Batalha N.M., Vogt S.S., 1999, ApJS 123, 251
Strassmeier K.G., Fekel F.C., Bopp B.W., Dempsey R.C., Henry G.W., 1990, ApJS 72, 191
Strassmeier K.G., Rice J.B., Wehlau W.H., Hill G.M., Matthews J.M., 1993, A&A 268, 671
Strassmeier K.G., 1994, A&A 281, 395
Vaughan A.H., Baliunas S.L., Middelkoop F., et al., 1981, ApJ 250, 276
Wilson O.C., 1968, ApJ 153, 221
Wilson O.C., 1978, ApJ 226, 379
Zarro D.M., Rodgers A.W., 1983, ApJS 53, 815
Zirin H., 1988, Astrophysics of the Sun. Cambridge Univ. Press, Cambridge, UK